

Fully converged time-dependent Hartree-Fock results for He^{2+} -He: Correlation in inclusive charge transfer

K. J. Schaudt, N. H. Kwong, and J. D. Garcia

Department of Physics, University of Arizona, Tucson, Arizona 85721

(Received 4 October 1990)

Previous time-dependent Hartree-Fock (TDHF) calculations of collisions between He ions and He atoms have been extended with improved accuracy. New features include using a Hermitian Coriolis term and installing classical quantum coupling, which allows completely self-consistent treatment of both the nuclear and electronic coordinates. Increased computer capabilities have allowed us to eliminate previous numerical limitations. We have calculated the single- and double-capture cross sections in the energy range of 1 to 250 keV. Comparison with experiments allows us to investigate the strengths and weaknesses of TDHF theory. Since correlation is best defined to be that which is not included in single-particle descriptions, we discuss converged results with regard to what they reveal about correlation.

INTRODUCTION

The well-known difficulties hindering a proper theoretical treatment of ion-atom collisions arise from the short duration, strong nonlinear interactions between the components, as well as the rearrangement of the constituents. Our approach to addressing these difficulties has been the adaptation of time-dependent Hartree-Fock (TDHF) theory.¹ Other methods applied to ion-atom collisions are based on expansions in molecular or atomic state basis.^{2,3} However, these methods are limited in the range of energy over which each method is applicable. The molecular state basis expansion gives reasonable results for energies below ~ 100 keV, while the atomic state basis expansion gives reasonable results above ~ 200 keV. In our previous work on He^{2+} and He collisions at 30 and 250 keV, we found that we could bridge the gap between the energies at which molecular and atomic state expansions are applicable. Our then-limited computing resources, however, imposed various numerical truncations, the effects of which were not checked. There were also some formulational problems, as explained below. Thus, although we have confidence in the general validity of our old results, which were in good agreement with experiments, we were not ready to assess quantitatively the strengths and weaknesses of the TDHF theory. Since the publication of Ref. 1, TDHF has been successfully applied to a variety of collision phenomena,⁴⁻⁸ so that its usefulness in providing qualitative insights into multiple-electron dynamics is no longer in doubt. Yet many currently debated issues, such as the significance of correlations, can be rigorously addressed only when the theory's numerical uncertainties are under control. This end has been achieved in the past several years through an increase of the computing power available to us and improvements in the formulation. As the first of a series of applications, we have repeated and extended the He^{2+} -He charge-transfer calculations of Ref. 1. This paper reports a rather detailed comparison of our results

with experiments, as well as other theories, and discusses the understanding gained toward the reaction mechanisms from such a comparison.

In Sec. II, we discuss the improvements and their effects on the numerical accuracy of our results. The improvements include (i) ensuring saturation in the size of the calculation box, the expansion in the azimuthal quantum number, and the number of final states used for projection; (ii) using a Hermitian discretization of the Coriolis term; and (iii) introducing a consistent coupling of the nuclear and electronic motions at lower energies. Adding the fluctuations due to the equation's nonlinearity, the results we present in Sec. III have uncertainties of less than 10%. In general, the improvements tend to confirm the results of the original calculations, showing the robust nature of the TDHF method as applied to atomic collisions. However, the extended range and controlled accuracy of our present results allow a more complete discussion of the physics. We compare our single- and double-capture cross sections with experiments and two standard basis expansion calculations over the range of 1 to 250 keV. The match at intermediate energies is good, while distinct discrepancies exist below ~ 20 keV. These are interpreted in terms of the degree of adequacy of the single particle (mean-field) picture. In Sec. IV, we conclude with some remarks on how TDHF bears on the definition and experimental demonstration of correlations and the implications of our results on other systems.

THEORY AND IMPROVEMENTS

Time-dependent Hartree-Fock theory produces the best possible wave functions for a given Hamiltonian which are Slater determinants of single-particle orbitals. In most ion-atom collisions, as in this case, approximate cylindrical symmetry is present. The reference frame rotates along with the internuclear axis to take advantage of this cylindrical symmetry and to reduce the calculational load. This rotation introduces a Coriolis term

($\omega\hat{L}_y$), which couples states having m values which differ by one unit. An expansion involving states with definite m value is then performed. This expansion in m must be large enough to include the full effects of the Coriolis term. In our first improvement we have extended the m expansion capability of the program to include all m , and have actually kept terms through $m=2$.

The TDHF equations in the rotating frame in cylindrical coordinates were laid out in Ref. 1. We solve the equations using finite differences with zero boundary conditions. The advantages of using this method, such as the automatic inclusion of continuum states during the collision have been discussed in previous papers.^{9,10} Previous technical difficulties arising from a non-Hermitian discretization of the Coriolis term have been corrected. The manifestly Hermitian discretized form in use now is given in the Appendix. The grid wave function is propagated in time by the Peaceman-Rachford scheme and transition probabilities are computed by projection onto specified final states.

The size of the ‘‘box’’ in which we carry out our calculations can have an effect on the results due to the fact that the boundary reflects the wave function. Therefore the box must be large enough that the reflections are negligible. In our third improvement, we have increased the box size from $4 \text{ \AA} \times 13 \text{ \AA}$ to $8 \text{ \AA} \times 20 \text{ \AA}$. The fourth improvement involves the increase of the number of bound states used during the projection on the evolved wave function. The previous calculations used only $1s$ to $2p$ for single capture and $1s^2$ to $1s2p$ for double capture, we have now expanded to $4f$ in single capture and to $1s4f$ in double capture. For each excited two-electron state we use a ten-parameter Slater-orbital fit to the standard Herman-Skillman state. The values of the parameters were listed in Ref. 9.

Orbitals of $m \leq 1$ were included in the previous calculation. The effect of including additional m is less than 10% at 250 keV and is smaller at lower energies. The inclusion of the $3s$ to $4f$ states in the final-state projections again added at most a few percent. Increasing the box size (area covered) by 200% had approximately a 2% effect on double capture and a 5% effect on single capture. Because the difference between the small and big box were small, we used a medium sized box $\sim 75\%$ larger than the small box to save on computer time for a majority of the calculations.

Adding up these numerical uncertainties, we determine an upper bound of 10% for the possible deviation of our result from that which an exact solution of the TDHF equations would yield. Owing to the nonlinearity of the equations, the projection probabilities may oscillate at asymptotic time. The amplitude of these oscillations was found to be no more than 5% of the value at minimum; furthermore, such oscillations occur at only a few, if any, values of the impact parameter over the entire calculation. In these cases, we take the predicted value for the probability to be the average value. Because these oscillations occur over only a small range of impact parameters, the overall uncertainty contributed by the nonlinearity of the TDHF equations is less than 1%. As discussed in Sec. IV, larger deviations from established experimen-

tal data may be attributed to correlation between the two electrons.

In atomic collisions we can treat the heavier particles, the nuclei, classically and the lighter particles, the electrons, quantum mechanically. In Ref. 1, the electrons responded to the presence of the moving nuclei and the other electrons, however, the nuclei responded only to the presence of the other nucleus. Classical quantum coupling (CQC), our fourth improvement, allows the nuclei to respond to the presence of the electrons as well. In the rotating frame the variational solution based on the least-action principle gives

$$\delta \int dt \left\langle \psi \left| i\hbar \frac{\partial}{\partial t} - (\hat{H} - \omega\hat{L}_y) \right| \psi \right\rangle = 0, \quad (1a)$$

where

$$\hat{H} = - \sum_i^N \frac{\hbar^2}{2M_i} \nabla_{\mathbf{X}_i}^2 + \sum_{i(<j)}^N V_{nn}(\mathbf{X}_i, \mathbf{X}_j) + \hat{H}_e(\mathbf{X}_i, \dots, \mathbf{X}_N, \dots, \mathbf{x}_i, \dots, \mathbf{x}_A) \quad (1b)$$

and

$$\hat{H}_e = \sum_i^A \frac{\hbar^2}{2m} \nabla_{\mathbf{x}_i}^2 + \sum_i^A \sum_j^N V_{en}(\mathbf{X}_j, \mathbf{x}_i) + \sum_{i(<j)}^A V_{ee}(\mathbf{x}_i, \mathbf{x}_j), \quad (1c)$$

where V_{ab} denote the interaction between particles a and b , the \mathbf{X}_i , $i=1, \dots, N$, are the nuclear coordinates and \mathbf{x}_i , $i=1, \dots, A$, denote the electron coordinates. Using the WKB approximation for the nuclear coordinates allows us to obtain the following equations of motion, as shown in Ref. 11:

$$i\hbar \frac{\partial \psi}{\partial t} = \hat{H}_e \psi(\mathbf{x}_i, \dots, \mathbf{x}_A, t), \quad (2a)$$

$$\dot{\mathbf{X}}_j = \mathbf{P}_j / M_j, \quad (2b)$$

$$\dot{\mathbf{P}}_j = - \sum_{i(\neq j)}^N \nabla_{\mathbf{X}_j} V_{nn}(\mathbf{X}_i(t), \mathbf{X}_j(t)) - \sum_i^A \langle \psi | \nabla_{\mathbf{X}_j} V_{en}(\mathbf{X}_j, \mathbf{x}_i) | \psi \rangle, \quad (2c)$$

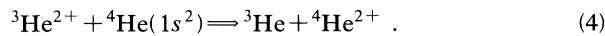
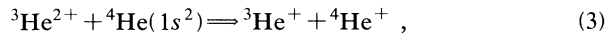
where ψ describes the wave function associated with the electrons. The second term in Eq. (2c) is the term produced by CQC. Equations (2a)–(2c) are now completely self-consistent and provide for the the conservation of total energy and total linear and angular momentum. In our scheme, Eq. (2a) is further approximated by the TDHF equation. As discussed more fully in the following section, the correction due to CQC is appreciable only for $E \lesssim 1$ keV.

RESULTS AND DISCUSSIONS

We calculated the single- and double-capture cross sections, whose processes are defined in Eqs. (3) and (4), respectively, for energies ranging from 1 to 250 keV:

TABLE I. Parameters for our current results are as follows: m expansion to $m=1$, box size is medium ($6 \text{ \AA} \times 15 \text{ \AA}$), no CQC, final projection state up to $1s2p$ for double capture and up to $2p$ for single capture unless otherwise noted in the comments column.

Energy (keV)	Double capture (\AA^2)	Single capture (\AA^2)	Comments
1	1.35	0.531	
1	1.49	0.580	with CQC
5	1.59	0.695	
10	1.60	0.921	
30	1.53	1.34	big box ($8 \text{ \AA} \times 20 \text{ \AA}$), with CQC
50	1.22	1.76	
100	0.887	1.81	$m=2$
150	0.622	1.70	$m=2$
250	0.229	0.978	$m=2$, big box



The results are tabulated in Table I.

In Figs. 1 and 2, we compare our results with the cross sections measured by several experimental groups^{12–16} and results from two standard basis expansion calculations.^{2,3}

Our double-capture cross sections agree very well with available experimental results over the range of 30 to 350 keV (Fig. 1). Below ~ 30 keV, our results show a leveling off of the double-capture cross section, which appears to be in agreement with the experimental data of Berkner *et al.*¹² However, their lowest energy was only 7.2 keV. Experimental data below 10 keV are scarce. The data of Afrosimov *et al.*¹³, which go down to ~ 1 keV, show a

definite rise as the energy is decreased below 10 keV. This rise has been predicted by molecular-orbital calculations by Harel and Salin² and is consistent with an adiabatic resonant reaction.¹⁷ Other experimental data^{14–16} either have no or few results below 10 keV and their data do not clearly indicate either a rise or leveling off below 10 keV. It should also be noted that some of the experimental data of different groups do not agree (errors included). As Bayfield and Khayrallah¹⁵ point out, there appears to be a need for more experiments to determine a standard cross section for He^{2+} -He collisions.

Our results for single capture are in good agreement with Afrosimov *et al.*¹³ and Allison¹⁴ over the energy ranges ~ 30 to 250 keV (see Fig. 2), the point at 250 keV slightly underestimating the experimental cross section. However, our results are high for energies ~ 10 keV with respect to all the experimental data.

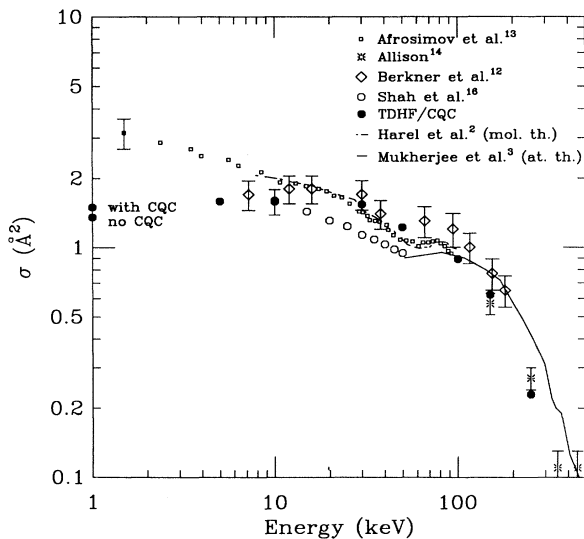


FIG. 1. Total cross section for double charge transfer vs incident energy in He^{2+} -He collision.

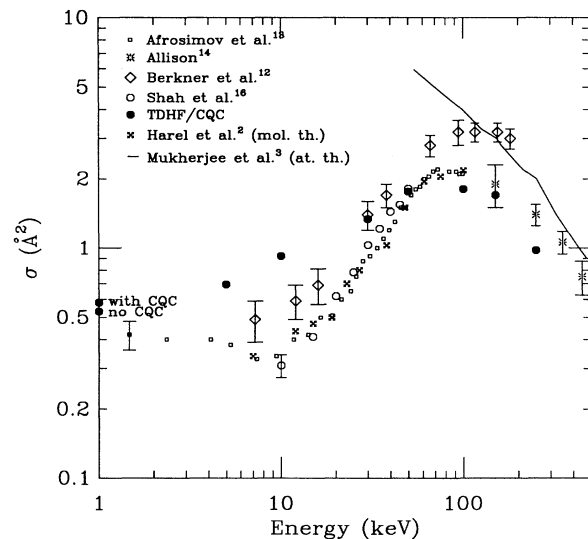


FIG. 2. Total cross section for single charge transfer vs incident energy in He^{2+} -He collision.

We begin the interpretation of our results with a brief discussion of the consequences of restricting the two-electron wave function to a Slater determinant. In the spin-singlet channel, the coordinate space wave function is a product of two identical single-particle orbitals. If P_2 is the asymptotic overlap probability of this single-particle orbital with Hartree-Fock orbitals around the projectile ion, the double-capture probability is roughly P_2^2 . Similarly, if P_1 is the overlap probability with hydrogenic orbitals, the single-capture probability is $\lesssim 2P_1(1-P_1)$. Now since the Hartree-Fock orbitals and hydrogenic orbitals—at least the low-lying ones—are geometrically similar, P_1 and P_2 are approximately equal. Heuristically, then, TDHF calculates the charge distribution, which is distributed statistically into various channels for the calculation of cross sections. At intermediate energies, when many channels are open, the quantitative agreement of our results with experiments is evidence that single-electron dynamics, containing only information about the motion of the nuclei and the changing charge distribution of the other electron, is the dominating factor.

The same product nature of the TDHF wave function causes problems below 30 keV, which can be more clearly elucidated with the help of the state resolved data of Afrosimov *et al.*¹⁸ In this experiment they found that, at low energies, one-electron capture is dominated by capture into states with $n \geq 2$. This they explained by a near-adiabatic model of transitions as the internuclear distance decreases from infinity to the united atom limit. The computed adiabatic potential curve¹⁹ for the channel $\text{He}^+(1s) + \text{He}^+(1s)$ is far from the incoming potential curve for $\text{He}^{2+} + \text{He}(1s^2)$ in most internuclear distances, while the potential curves for $\text{He}^+(1s) + \text{He}^+(n \geq 2)$ lie near and cross the incoming potential curve. Consequently, the capture into $\text{He}^+(1s)$ is suppressed at low energies. This suppression, together with the resonant capture into $\text{He}(1s^2)$, is inconsistent with the statistical relation between the single-capture and double-capture probabilities inherent in TDHF considered above. More precisely, at low energies, the mean-field charge overlap probability with the $1s$ orbital $P_1 \sim P_2 = P$ typically oscillates with large amplitude as a function of the impact parameter out to a certain radius. The single-capture probability to $\text{He}^+(1s)$, being $\sim 2P(1-P)$, is thus sizable on the average, which leads to an overestimation of the single-capture cross section. For example, the data of Afrosimov *et al.*¹⁸ show at 10 keV $\sim 10\%$ and at 5 keV only $\sim 0.05\%$ of single capture is into the $1s$ state, while TDHF calculation puts over 90% of the single capture in the $1s$ state. Since ionization is negligible, unitarity imposes a corresponding shortfall in the double-capture cross section.

The introduction of CQC can be seen in the capture cross section at 1 keV where it produces an increase in both single and double capture of 9–10%; it is negligible at higher energies. This increase is due to a shifting of the cross-section peaks and troughs toward larger b in the presence of CQC. This can be understood in terms of the work by Lichten.²⁰ When the atom and ion are close enough to interact, there is oscillation of the charges be-

tween the two nuclei at the frequency of E/h , where E is the energy difference between the symmetric and antisymmetric wave functions. The effect of CQC slows the nuclei, so at the same impact parameter the collision with CQC included spends more time in the interaction region. To spend the same amount of time in the interaction region, the impact parameter must be larger.

CONCLUSION

Correlation effects are generally understood to be experimental results that cannot be interpreted in an independent electron picture. Disagreement exists, however, as to how one should split the electron-electron interaction into single-particle and correlation terms.^{21–23} The standard definition of correlation is adopted by Stolterfoht²³ as being the differences between the exact transition probabilities and those predicted by TDHF. This definition has the obvious merit of including as much of the dynamics as can be quantitatively defined—via a variational principle—in the time-dependent screening mean field. Especially in complicated and confusing situations, the comparison of TDHF with experiment can isolate correlation effects in a physically and operationally unambiguous way. For this purpose, estimates on the numerical uncertainties of the TDHF predictions must be sharper than are adequate for drawing qualitative insights. Other choices for the definition of correlation are more arbitrary (even though Stolterfoht,²³ ultimately, rejected TDHF as a practical analytical tool because of its difficulty of implementation). We show, in this paper, how TDHF can be applied in this quantitative way. To within 10% uncertainty, our results show that at intermediate energies the evolving screening charge cloud is a good physical picture in the interpretation of inclusive single-capture and double-capture data. They also show that correlation effects in these cross sections are measurable at low energies and that they reflect the failure of TDHF to account for the suppression of *single* capture into $\text{He}^+(1s)$. Although this molecular-orbital correlation is rather trivial and well understood,¹⁸ this example serves as a reminder that correlation may still surface in single-electron transition amplitudes. For $E \gtrsim 250$ keV, we feel that there are too few data available to draw any firm conclusions.

This study of the relative importance of the mean field and correlation will be carried out for other two-electron systems. The implementation of a continuum wavefunction energy projection operator is under way which will extend our analysis to ionization processes. It also allows us to follow the change of the energy distributions (in addition to the spatial charge distributions) during the collision. The linear growth of computing workload with the number of electrons should make TDHF and its extensions very competitive in describing heavier systems. There TDHF can still be used to separate the effects of the mean field and correlations in inclusive transition data. Moreover, interesting collective effects may emerge from the charge and energy distributions given by the

mean field.

The effect due to a consistent classical-quantal coupling is only felt at 1 keV, where correlation is already much more important. We would like to mention, however, an application where CQC is essential. In our calculation of muon capture by helium reported elsewhere,⁹ CQC provides the sole mechanism for energy exchange between the classical muon and the quantal (TDHF) electrons, and CQC-TDHF is the most realistic existing scheme in treating that capture process.

ACKNOWLEDGMENTS

This work was supported in part by the National Science Foundation through Grant No. PHY9014797.

APPENDIX

One defect of earlier versions¹ was a non-Hermitian discretized Coriolis term that was capable of causing instabilities under relatively "benign" conditions. This defect has now been corrected and the Hermitian discretized Coriolis term in the action is

$$\begin{aligned} \langle \psi | \hat{L}_y | \psi \rangle = & \sum_{\mu, j, k} \Delta z \Delta \rho \frac{i\hbar}{2} \left\{ \frac{\rho_j}{2\Delta z} \left[g_{jk}^{\mu*} g_{j,k+1}^{\mu-1} - g_{j,k+1}^{\mu*} g_{jk}^{\mu-1} \right] + [(\mu-1) \rightarrow (\mu+1)] \right. \\ & - \frac{z_K}{2\Delta \rho} \left[\frac{\rho_j + \frac{1}{2}}{\sqrt{\rho_{j+1}\rho_j}} \left[g_{jk}^{\mu*} g_{j+1,k}^{\mu-1} - g_{j+1,k}^{\mu*} g_{jk}^{\mu-1} - \frac{\Delta \rho}{\rho_j} g_{jk}^{\mu*} g_{jk}^{\mu-1} \right] \right] \\ & \left. - [(\mu-1) \rightarrow (\mu+1)] + \frac{z_k}{\rho_j} [(\mu-1) g_{jk}^{\mu*} g_{jk}^{\mu-1} - (\mu+1) g_{jk}^{\mu*} g_{jk}^{\mu+1}] \right\} \end{aligned} \quad (A1)$$

where $[(\mu-1) \rightarrow (\mu+1)]$ denotes a term that is the same as the previous one with $\mu-1$ replaced by $\mu+1$, and where $g_{jk}^{\mu} \equiv \sqrt{2\pi\rho_j} \psi_{jk}^{\mu}$, where μ is the azimuthal quantum number and j and k define, respectively, the r and z grid point number. This yields the following term in the Euler-Lagrange (TDHF) equation:

$$\begin{aligned} \frac{1}{\Delta \rho \Delta z} \frac{\partial \langle \psi | \hat{L}_y | \psi \rangle}{\partial g_{jk}^{\mu*}} = & \frac{i\hbar}{4} \left[\frac{\rho_i}{\Delta z} \left[g_{j,k+1}^{\mu-1} - g_{j,k-1}^{\mu-1} + g_{j,k+1}^{\mu+1} - g_{j,k-1}^{\mu+1} \right] \right. \\ & - \frac{z_k}{\Delta \rho} \left[C_j g_{j+1,k}^{\mu-1} - C_{j-1} g_{j-1,k}^{\mu-1} + C_j g_{j+1,k}^{\mu+1} - C_{j-1} g_{j-1,k}^{\mu+1} \right] \\ & \left. + \frac{z_k}{\rho_j} [(2\mu-1) g_{jk}^{\mu-1} - (2\mu+1) g_{jk}^{\mu+1}] \right], \end{aligned} \quad (A2)$$

where

$$C_j = \frac{j}{(j^2 + \frac{1}{4})^{1/2}}.$$

Put in matrix form, labeled by (μ, j, k) , this term may easily be verified to be Hermitian for any value of M , where $\mu=0, 1, \dots, M$. More details can be found in Ref. 9.

¹K. R. Sandhya Devi and J. D. Garcia, *J. Phys. B* **16**, 2837 (1983); K. R. Sandhya Devi and J. D. Garcia, *Phys. A* **30**, 600 (1984).

²C. Harel and A. Salin, *J. Phys. B* **13**, 785 (1980).

³S. C. Mukherjee, K. Roy, and N. C. Sil, *J. Phys. B* **6**, 467 (1973).

⁴K. C. Kulander, *Phys. Rev. A* **36**, 2726 (1987).

⁵D. Tiszauer and K. C. Kulander, *Phys. Rev. A* **29**, 2909 (1984).

⁶K. J. Schafer, N. H. Kwong, and J. D. Garcia, *Comput. Phys. Commun.* (to be published).

⁷C. Bottcher, *Nucl. Instrum. Methods Phys. Res. B* **10/11**, 7 (1985).

⁸K. Gramlich, N. Grün, and W. Scheid, *J. Phys. B* **19**, 1457 (1986).

⁹N. H. Kwong, K. J. Schaudt, and J. D. Garcia, *Comput. Phys. Commun.* (to be published).

¹⁰J. D. Garcia, *Nucl. Instrum. Methods Phys. Res. A* **240**, 552 (1985).

¹¹N. H. Kwong, *J. Phys. B* **20**, L647 (1987).

¹²K. H. Berkner, R. V. Pyle, J. W. Stearns, and J. C. Warren, *Phys. Rev.* **166**, 44 (1968).

¹³V. V. Afrosimov, G. A. Leiko, Y. A. Momaev, and M. N. Panov, *Zh. Eksp. Teor. Fiz.* **67**, 1329 (1974) [*Sov. Phys.—JETP* **40**, 661 (1975)].

¹⁴S. K. Allison, *Phys. Rev.* **109**, 76 (1958).

¹⁵J. E. Bayfield and G. A. Khayrallah, *Phys. Rev. A* **11**, 920 (1975).

¹⁶M. B. Shah and H. B. Gilbody, *J. Phys. B* **7**, 256 (1974).

¹⁷A. F. Ferguson and B. L. Moiseiwitsch, *Proc. Phys. Soc. London* **74**, 457 (1959).

¹⁸V. V. Afrosimov, A. A. Basalae, G. A. Leiko, and M. N. Panov, *Zh. Eksp. Teor. Fiz.* **74**, 13 (1978) [*Sov. Phys.—JETP* **74**, 13 (1978)].

- 47, 6 (1978)].
- ¹⁹V. K. Nikulin and N. A. Gashchina, *Zh. Tekh. Fiz.* **48**, 13 (1978) [*Sov. Phys.—Tech. Phys.* **23**, 7 (1978)].
- ²⁰W. Lichten, *Phys. Rev.* **131**, 1 (1963); **131**, 229 (1963).
- ²¹J. H. McGuire, *Phys. Rev. A* **36**, 114 (1987).
- ²²J. F. Reading and A. L. Ford, *Invited Papers of the International Conference on the Physics of Electronic and Atomic Collisions*, edited by H. B. Gilbody, W. R. Newell, F. H. Read, and A. C. Smith (North-Holland, Amsterdam, 1988), p. 693.
- ²³N. Stolterfoht, in *Conference on the Spectroscopy and Collision of Few Electron Ions, Bucharest, 1989*, edited by V. Floreanu and V. Zoran (World Scientific, Singapore, 1989).